

ENC-2020-0794

EVALUATION OF SMD EFFECTS ON CHARACTERISTIC LENGTHS OF  
LIQUID ROCKET ENGINES USING ETHANOL/LOX AND RP-1/LOX

**Maurício Sá Gontijo**

Department of Aerospace Engineering, University of Brasília, St. Leste Projeção A - Gama Leste Brasília - DF 72444-240, Brazil  
[mauricio.sa.gontijo@gmail.com](mailto:mauricio.sa.gontijo@gmail.com)

**Gustavo Alexandre Achilles Fischer**

**Fernando de Souza Costa**

Combustion and Propulsion Laboratory - LABCP, National Institute for Space Research - INPE, Rodovia Presidente Dutra, km 40, CEP 12630-000, Cachoeira Paulista/SP - Brazil  
[gustavo.achilles.fischer@gmail.com](mailto:gustavo.achilles.fischer@gmail.com)  
[fernando.costa@inpe.br](mailto:fernando.costa@inpe.br)

**Abstract.** Liquid propellant rocket engines are used in many aerospace applications, since they show higher performance than solid propellant motors and allow thrust control. The characteristic length ( $L^*$ ) is an important parameter for the combustion chamber design, and is related to the stay time required for propellants to fully atomize, mix and react within the rocket chamber. Injector design is also an important factor once it affects directly the droplet Sauter mean diameter (SMD), impacting on  $L^*$ . Pressure swirl injectors are widely used in propulsion applications because they can yield efficient atomization within a small volume. The swirl motion inside the injector creates a hollow cone spray, particular characteristic of this type of injector, decreasing  $L^*$ . Ethanol/LOx and RP-1/LOx are propellant combinations used historically in several liquid propellant rocket engines. This work presents a theoretical study of the  $L^*$  for these mixtures, based on Spalding model for droplet vaporization and combustion and the SMD models of Radcliffe and Jasuja. The algorithm was validated with data of three engines for chamber pressures from 10 to 250 bar and mixture ratios from 1 to 7. The Radcliffe model has predicted better the SMD for the  $L^*$  comparing with actual engines, and SMD has affected in about 58 % the  $L^*$ . Also, the concept of the characteristic equivalence ratio ( $\Phi^*$ ), which is the equivalence ratio ( $\Phi$ ) required to reach the minimum  $L^*$ , was presented. The results showed that, besides the thermo-physical properties of each fuel, the  $L^*$  decreases with the increase in chamber pressure, reduction in propellant mass flux and closer to characteristic equivalence ratio. In general, the  $L^*$  of the Ethanol/LOx is higher than the RP-1/LOx and it is reached with  $\Phi^*$  of about 0.779 and 1.632, respectively, which are values compatible to actual engines.

**Keywords:** Characteristic Length, Sauter Mean Diameter, Liquid Propellant Rocket Engines, Pressure Swirl Injectors,

**1. INTRODUCTION**

Liquid Propellant Rocket Engines (LPREs) are the most common propulsion systems used on launch vehicles and satellites worldwide due to its high performance and possibility thrust modulation. The combustion chamber design is highly dependent on the space required for the injection, atomization, mixing and combustion of the propellants. This space is represented by the characteristic length. Since it is a parameter that depends on the propellants and injector properties, in general, books and other works present only empirical data for some pairs. But it is not informed on which conditions the tests were performed (Huzel and Huang, 1992), (Humble et al., 1995). Therefore, a theoretical model to describe the impact of the  $L^*$  in the combustion process and the thrust chamber geometry is crucial on the design of the engine, and by optimizing this parameter weight, costs, and performance losses are reduced significantly (Huzel and Huang, 1992). Equation (1) demonstrates how the  $L^*$  is substantial for the thrust chamber design, by being a relation between the chamber volume,  $V_c$ , and the throat area,  $A_t$ .

$$L^* = \frac{V_c}{A_t} = \frac{\dot{m}Vt_s}{A_t} \quad (1)$$

where  $\dot{m}$  is the propellant mass flow rate,  $V$  is the average specific volume, and  $t_s$  is the residence time or stay time for the injection, atomization, mixing and combustion of the propellants. One of the first mathematical models to estimate the  $L^*$  was proposed by Spalding (1959), and it is until now being used, because it is a relatively simple one-dimensional model with analytical solution. Furthermore, it may contain chemical kinetics effects considerations, like reactivity, being solved numerically. Other more complex models were also developed, they were compiled at (Salvador, 2004) who also proposed a new approach (Salvador and Costa, 2006). But, all of these models need to be solved numerically, being computational and time costly.

Injection and atomization process are fundamentally important for the characteristic length. In general, rocket injectors are the jet or pressure swirl type, and variables related to liquid characteristics (injection velocity, drop size, etc.) need experimental data or empirical, or semi-empirical, equations specific to each type of injector. Some models or empirical equations helps to determine some variables used on  $L^*$  calculation, some of these are encountered on (Lefebvre and McDonell, 2017). The evaporation, responsible for the atomization, is the slowest process, that's why so many models focus on modelling so accurately this phase. This work studied pressure swirl injectors, because they are widely applied on rocket engines and there are many theoretical, numerical, and experimental studies characterizing these injectors (Fischer 2014, 2019), (Fischer et al., 2017).

The droplet size is determined by the Sauter mean diameter (*SMD*). It is a parameter that represents the ratio of the volume to the surface area of the spray, highly used on applications with liquid fuels combustion systems (Lefebvre and McDonell, 2017). It has great impact on the  $L^*$ , since the bigger the droplet, the higher is the time for the droplets to evaporate. This happens because small droplets augment the surface area of the fluid, increasing evaporations rates (Bayvel and Orzechowski, 1993), (Khavkin, 2003), (Bazarov et al., 2004), (Wang, 2016).

In the Brazilian space program, there is a significant interest in developing a LPRE for its Microsatellite Launch Vehicle (VLM) last stage. A mixture of liquid oxygen (LOx) and ethanol is being researched and two small engines were developed, the L5 (5 kN) and the L15 (15 kN), and a third and bigger one, the L75 (75 kN) (Torres et al., 2009), (Pfuetzenreuter et al., 2017). The  $L^*$  optimization would improve in a significant way the project and its feasibility. This mixture was one of the first used by the V-2 rocket back in the 40's. Also, the RP-1 was the first choice for the L75 engine due to its high efficiency and it is used in several launch vehicles.

In all of these Brazilian engines, pressure swirl injectors were used. This type of injectors consists of tangential inlet orifices, vortice/swirl chamber, convergent section and discharge orifice. It is imposed a swirl motion to the propellant due to the tangential orifices and conservation of angular momentum creating an air core, developing a hollow conical swirling film flowing out of the injector and creating a wide spray cone angle. This results in low discharge coefficient and on a finer atomization directly proportional to the opening of the spray cone angle. With the geometrical design parameters, it is possible to determine or adjust the spray cone angle, mass flow rate, breakup lengths, *SMD*, axial and tangential velocities and atomization parameters (Schmidt and Walzel, 1984), (Rizk and Lefebvre, 1985), (Bayvel and Orzechowski, 1993), (Ashgriz, 2011), (Saeedipour et al., 2014), (Vijay et al., 2015), (Kang et al., 2018).

This work intends to make a theoretical study of the  $L^*$  for two different propellant combinations, Ethanol/LOx and RP-1/LOx, varying some engine properties that may impact on the characteristic length results. Two ranges of chamber pressure were analyzed, the first one from 10 to 70 bar, due to a large number of small LPREs operating in these ranges, such as the three Brazilian ones cited before, and some high thrust engines such as the RD-108, with 51 bar (Haidn, 2008), the engine from V-2 (Aggregat 4 - A4) that had around 15 bar (Spalding, 1959). The second range is from 70 to 250 with motors such as the F-1 engine from Saturn V, NK-33 and RD-170 that had around 77.6 bar, 145.4 bar and 251 bar, respectively (Hugh, 1995), (Hulka et al., 1998), (Haidn, 2008). All of these engines operated with mixtures of Ethanol/LOx or RP-1/LOx.

## 2. THEORETICAL MODEL

The Spalding's model (Spalding, 1959), as mentioned by Hill and Peterson (1992), considers an idealized cylindrical combustion chamber, with a uniform size droplet with uniform velocity, and drops of fuel and oxidizer are indistinct. Other assumptions are that it is considered a one-dimensional flow, the gas composition is at equilibrium, the time required for the vaporization is the time required for combustion, chamber pressure and temperature are uniform, and droplets are spherical.

The drag actuated on spherical particles are represented on the equation below:

$$S = \frac{9Pr}{2\ln(1+B)} \approx \frac{9Pr}{2B} \quad (2)$$

where  $B$  is the transfer number and  $Pr$  is the Prandtl number, which is around 0.7. In this work it is calculated with a NASA's software CEA (Chemical Equilibrium with Applications) (Mcbride and Gordon, 1994, 1996), but it can be calculated as:

$$Pr = \frac{c_p \mu}{k} \quad (3)$$

where  $c_p$  is the specific heat of gaseous combustion products with constant pressure,  $\mu$  is the dynamic viscosity, and  $k$  is the thermal conductivity. According to Spalding (1959), values of  $S$  should be close to 0.5.

The transfer number, or Spalding number, is divided into four types (Spalding, 1953, 1979). The first and the second are the ones used on combustion of carbons and combustion of metals, respectively, and are not used in this model. The third transfer number is for combustion of liquid fuels and is the one used in this model. This third number is presented in Eq. (4).

$$B = \frac{H m_o}{Q r} + c_{pL} \frac{(T_g - T_s)}{Q} \quad (4)$$

where  $H$  is the calorific value of fuel,  $Q$  is the heat of vaporization,  $m_o$  is the weight concentration of oxygen,  $r$  is the weight of oxygen required for combustion of unit weight fuel,  $T_g$  is the gas stream temperature, and  $T_s$  is the temperature of the surface engaging in mass transfer.

The fourth is divided in two others, the transfer number by heat and by mass, which are used on vaporization models without combustion, such as the ones demonstrated on (Wang, 2016). The Spalding number by mass and by heat are equal if the Lewis number, that is the ratio of the thermal diffusivity to the mass diffusivity, is equal to 1. These two numbers are presented on Eqs. (5a) and (5b).

$$B_T = c_{pL} \frac{(T_g - T_s)}{Q} \quad (5a)$$

$$B_M = \frac{Y_s - Y_f}{1 - Y_s} \quad (5b)$$

where  $Y_s$  is the total propellant mass flow rate divided by fuel mass flow rate, and  $Y$  is the vapor mass fraction.

According to Spalding (1959), values of  $B$  should be close to 6 for bi-propellants.

The injection velocity has a high impact on the characteristic length, and depends on a pressure drop at the injector. Larger pressure drops provide better atomization (Schmidt and Walzel, 1984), (Saeedipour et al., 2014), and smooths pressure oscillations associated with combustion instabilities coupled with the feed system. But it also increases the  $L^*$  because it rises the injection velocity (Hill and Peterson, 1992). Therefore, higher pressure drops decrease the  $SMD$ , reducing the  $L^*$ . According to Sutton and Biblarz (2010), that pressure drop is of about 0.15 to 0.25 times the chamber pressure. Although, this pressure drop may vary with the chamber pressure, due to the fact that high pressure engines must have high pressure drop, hence the pressure oscillations may increase with the chamber pressure. The pressure drop can be calculated with the relation proposed by Humble et al. (1995), that is 30 % of the chamber pressure, but the relation proposed by Kessaev, on the internal report of the Brazilian Institute of Aeronautics and Space (IAE) and discussed by Mota et al. (2018), is a better approximation and it is presented at Eq. (6).

$$\Delta P = 80 \sqrt{10 P_C} \quad (6)$$

where  $P_C$  is the chamber pressure and is given in Pa.

With the pressure drop, the injection velocity is calculated as:

$$u_0 = \sqrt{\frac{2 \Delta P}{\rho_L}} \quad (7)$$

where  $\rho_L$  is the liquid fuel density.

With the injection velocity, it is possible to calculate the mass flow rate, which is defined as:

$$\dot{m}_L = C_d \rho_L u_0 A_{inj} \quad (8)$$

where  $C_d$  is the discharge coefficient, which is the theoretical mass flow rate divided by the experimental mass flow rate, representing the effectiveness of the injector. According to Sutton and Biblarz (2010), for pressure swirl injectors it can vary from 0.2 to 0.55.  $A_{inj}$  is the injection area of one injector, or the discharge area, and it depends on the orifice diameter that may vary from 1 to 6.4 mm for pressure swirl injectors.

The propellant mass flux in the combustion chamber is defined as the total propellant mass flow rate divided by the chamber area, as in Eq. (9).

$$G = \frac{\dot{m}_p}{A_C} \quad (9)$$

where  $A_C$  is the chamber area and  $\dot{m}_p$  is the total mass flow rate. The chamber area may depend on the number of injectors required (Kessaev, 1997).

Since pressure swirl injectors were used in this work, the Radcliffe model and the Jasuja model equations were implemented as shown in Eqs. (10) and (11) (Radcliffe, 1960), (Jasuja, 1979). These equations were chosen based on experimental data comparison made by (Fischer 2014, 2019) and (Fischer et al., 2017).

$$SMD = 7.3\sigma^{0.6}v_L^{0.2}\dot{m}_L^{0.25}\Delta P^{-0.4} \quad (10)$$

$$SMD = 4.4\sigma^{0.6}v_L^{0.16}\dot{m}_L^{0.22}\Delta P^{-0.43} \quad (11)$$

where  $\sigma$  is the surface tension,  $v_L$  is the kinematic viscosity,  $\dot{m}_L$  is the liquid fuel mass flow rate per injector.

The minimum, dimensionless, length for the propellant to evaporate is calculated as:

$$\xi^* = \frac{X_0 + 3S/10}{2+S} \quad (12)$$

where  $X_0$  is the ratio between the injection velocity and the final gas velocity at the nozzle inlet,  $X_0 = u_o/u_g$ . The final gas velocity at the nozzle inlet is calculated by using the finite area method that makes it possible to calculate the Mach number at this section of the engine, according to the contraction ratio, which can vary from 0.1 to 0.4 Mach inside the chamber (Humble et al., 1995) and may be calculated as shown in Eq. (13).

$$A_C/A_t = \frac{1}{M_C} \sqrt{\left\{ \frac{1 + [(\gamma-1)/2]M_C^2}{1 + [(\gamma-1)/2]} \right\}^{(\gamma+1)/(\gamma-1)}} \quad (13)$$

where  $\gamma$  is the ratio of specific heats and  $M_C$  is the Mach number at the nozzle inlet. With the  $M_C$ , the gas velocity is calculated as  $u_g = M_C(\gamma RT_C)^{1/2}$ , where  $T_C$  is the adiabatic flame temperature,  $R$  is the gas constant, expressed as  $R = R_0/M$ , in which  $R_0$  is the universal gas constant and  $M$  is the molecular weight of the combustion gas products.

Then, finally, the characteristic length can be calculated with Eq. (14).

$$L^* = \xi^* r_0^2 \left[ \frac{2}{\gamma+1} + \left( \frac{G}{\rho\sqrt{\gamma RT_C}} \right)^2 \frac{\gamma-1}{\gamma+1} \right]^{\frac{\gamma+1}{2(\gamma-1)}} \frac{c_p \rho_L \sqrt{\gamma RT_C}}{k \ln(1+B)} \quad (14)$$

where  $\rho$  is the density of the combustion products and  $r_0$  is the injected droplet radius, which is obtained by dividing the  $SMD$  by 2.

### 3. RESULTS AND DISCUSSIONS

A Matlab algorithm coupled with CEA to determine combustion properties was written to calculate the characteristic length of the engine and the results are presented in the following section. The finite area model was used to determine thermodynamic and transport properties at the nozzle inlet, assuming complete atomization, mixture and combustion of the propellants at this section of the engine.

The fuels properties are presented in Table 1 for anhydrous ethanol (Counsell et al., 1970), (Dong et al., 1987), (Gonçalves et al., 2010) and RP-1 (Chickos and Zhao, 2005), (Magee et al., 2007). The properties were obtained for 298.15 K and 1 atm (Mcbride and Gordon, 1992). The temperature of 90.15 K and pressure of 1 atm was used for the LOx thermophysical properties for the simulations (Mcbride and Gordon, 1994).

Table 1. Fuels properties (298.15 K and 1 atm)

Properties	Anhydrous Ethanol	RP-1
$\sigma$ (N/m)	0.0236	0.0280
$c_{pL}$ (J/kgK)	2.57	2.29
$v_L$ (m <sup>2</sup> /s)	1.402e-6	1.867e-6
$Q$ (J/kg)	841719.12	348413.23
$\rho_L$ (kg/m <sup>3</sup> )	788.3	799.1

Taking the A4 engine to validate the results, which has around 58 kg/s of ethanol mass flow rate on 1224 injector nozzles, around of 130 kg/s of total mass flow rate, chamber diameter of 0.922 m, throat diameter of 0.40 m, contraction ratio of 5.31, chamber pressure of 15 bar and pressure drop in the injector of around 2.34 bar, the algorithm reached 2.02 m and 1.35 m of characteristic length, using Radcliffe and Jasuja models respectively. According to Spalding (1959), the A4 has 2.87 m. Comparing both results, the algorithm demonstrated to be very efficient in predicting the  $L^*$ . It is important to mention that the Radcliffe and Jasuja models are for pressure swirl injectors, which are not the ones used in A4 and the simulation used anhydrous ethanol, but the A4 used 75 % v/v hydrous ethanol as fuel.

Furthermore, another validation test was made with an old version of the L75 engine, that used RP-1 instead of ethanol. It has 6.4 kg/s of RP-1 mass flow rate divided in 91 injectors, 22 kg/s of total mass flow rate, chamber diameter of 0.211 m, throat diameter of 0.090 m, contraction ratio of 5.49 and chamber pressure of 60 bar (Almeida et al., 1999). Also, the chamber length was published by Almeida et al. (1999) as 0.285 m, allowing to calculate the real  $L^*$  of 1.57 m. Running the simulations for this case it was obtained a  $L^*$  of 1.33 m and 0.79 m, using Radcliffe and Jasuja models respectively. For this case, the number of injectors was assumed as 91, the same as the recent version of the L75 engine, and the pressure drop calculated of 6.19 bar, using Eq. (6).

A third validation test was made with the F-1 engine that has 742 kg/s of RP-1 mass flow rate divided in 3700 injectors, 2526 kg/s of total mass flow rate, chamber diameter of 0.99 m, throat diameter of 0.915 m, contraction ratio of 1.17, chamber pressure of 77.6 bar, and 6.41 bar of pressure drop (Hugh, 1995). The pressure drop was calculated using the Eq. (6). Using Radcliffe and Jasuja models, were predicted 2.61 m and 1.39 m, which is close to the real characteristic length of 1.22 m. It is important to take in consideration that the F-1 engine didn't use pressure swirl injectors, so a more adequate *SMD* model should be used for this engine.

Figure 1 presents the results of *SMD* for Ethanol/LOx and RP-1/LOx, varying the chamber pressure from 10 to 250 bar and the correspondent pressure drop, using Radcliffe and Jasuja models. Figure 2 presents the results of  $L^*$  for Ethanol/LOx and RP-1/LOx, in terms of chamber pressure and varying the mixture ratio (*O/F*) from 1 to 7, using Radcliffe and Jasuja models. Figure 3 presents the results of  $L^*$  for Ethanol/LOx and RP-1/LOx, in terms of chamber pressure and varying the mixture ratio from 1 to 7, using Radcliffe and Jasuja models.

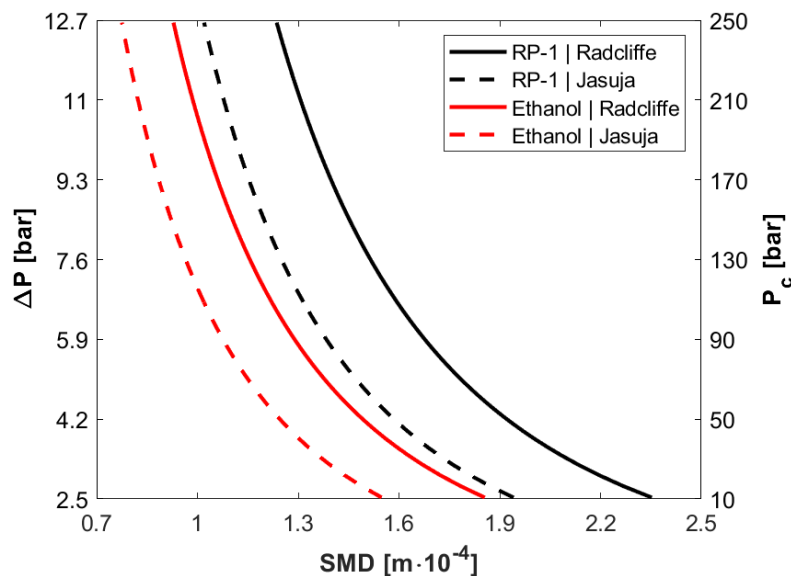


Figure 1. *SMD* for Ethanol/LOx and RP-1/LOx using Radcliffe and Jasuja models from 10 to 250 bar

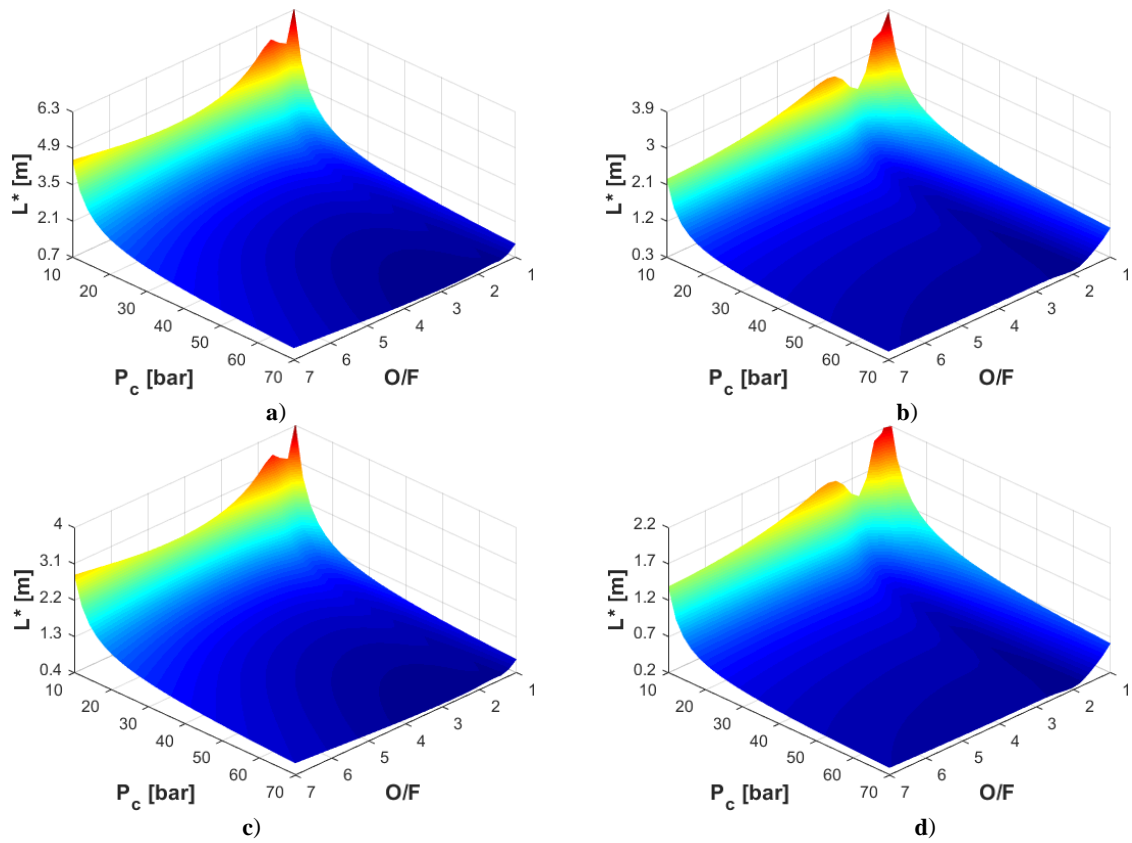


Figure 2. a)  $L^*$  for Ethanol/LOx using Radcliffe model, 10 to 70 bar; b)  $L^*$  for RP-1/LOx using Radcliffe model, 10 to 70 bar; c)  $L^*$  for Ethanol/LOx using Jasuja model, 10 to 70 bar; d)  $L^*$  for RP-1/LOx using Jasuja model, 10 to 70 bar

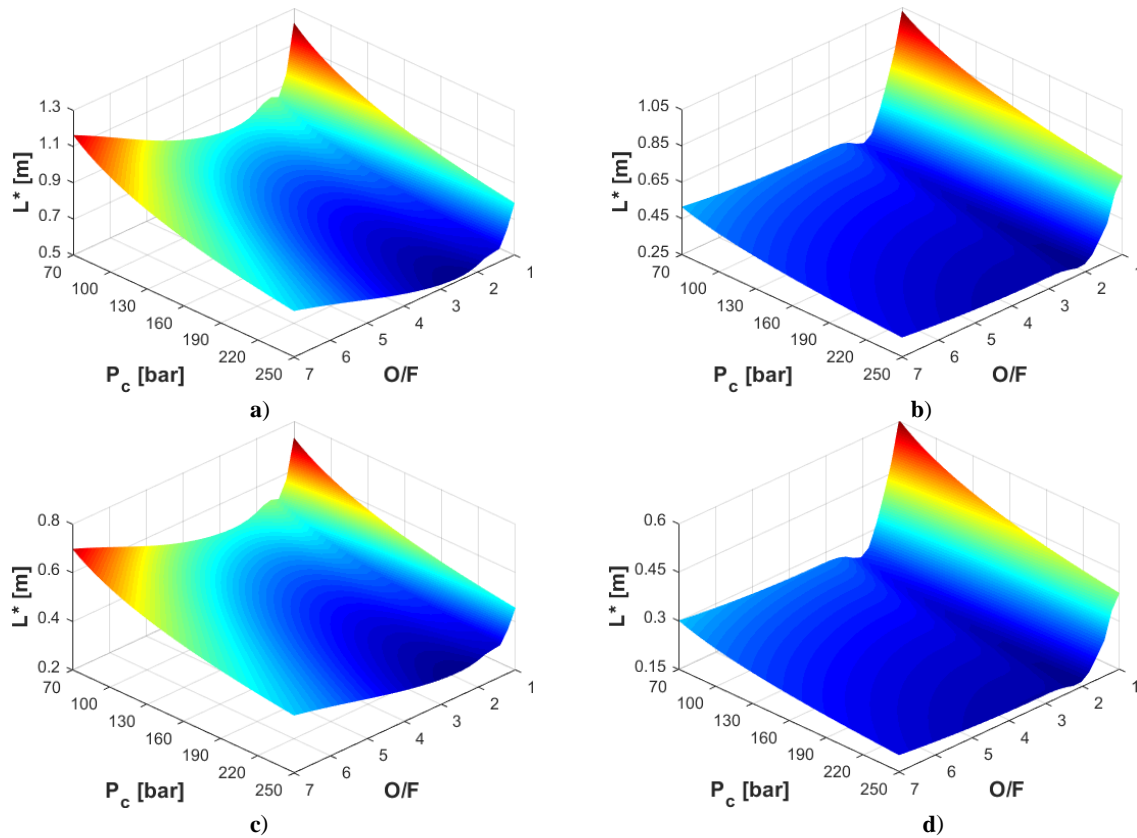


Figure 3. a)  $L^*$  for Ethanol/LOx using Radcliffe model, 70 to 250 bar; b)  $L^*$  for RP-1/LOx using Radcliffe model, 70 to 250 bar; c)  $L^*$  for Ethanol/LOx using Jasuja model, 70 to 250 bar; d)  $L^*$  for RP-1/LOx using Jasuja model, 70 to 250 bar

The results were obtained for the L75 engine that has around 8.85 kg/s of fuel mass flow rate in 91 pressure swirl injectors, around 22.95 kg/s of total mass flow rate (Pfuetzenreuter et al., 2017), chamber and throat diameter obtained through the mesh presented by Almeida 2013 of 0.088 m and 0.046, respectively, contraction ratio of 3.67, chamber pressure of 60 bar and the pressure drop of 6.19 bar, calculated using Eq. (6). The  $O/F$  ratio is the mass flow rate of oxidizer divided by the mass flow rate of fuel and represents the mixture between them. The equivalence ratio may also be analyzed to determine how close the mixture of propellants is to the stoichiometric mixture ratio. Eqs. (15) and (16) presents the mixture ratio and the equivalence ratio, respectively.

$$O/F = \frac{\dot{m}_{ox}}{\dot{m}_f} \quad (15)$$

$$\Phi = \frac{F/O}{(F/O)_{st}} \quad (16)$$

where  $\dot{m}_{ox}$  is the oxidizer mass flow rate,  $\dot{m}_f$  is the fuel mass flow rate,  $F/O$  is the inverse of the  $O/F$  ratio, and the subscript  $st$  defines the stoichiometric condition. Reaching a  $\Phi = 1$  is defined as the stoichiometric mixture, a  $\Phi > 1$  is defined as a fuel rich mixture, or rich mixture, and  $\Phi < 1$  is defined as a fuel lean mixture, or lean mixture.

As seen on Fig. 1 it is possible to verify that the  $L^*$  reduces as chamber pressure increases. The  $SMD$  also has high impact, and it varies with the chamber pressure due to the pressure drop, which varies with chamber pressure, as shown in Eq. (6) and Fig. 1.

Figure 4 improves the understanding of how each parameter affects the characteristic length. It is shown a pie flowchart representing the percentage of impact on the results. It is possible to observe that the injected droplet size, represented by the  $SMD$ , is the parameter that affects the most, the second most affecting parameter is the  $\xi^*$ , the third is the vaporization part, which is the inverse of the thermal diffusivity divided by a relation of the transfer number  $[(c_p \rho_L / k) / \ln(1+B)]$ , and the last is the gas dynamic part  $[(\gamma RT_c)^{1/2} \{2/(\gamma+1) + (G/(\rho(\gamma RT_c)^{1/2}))^2 (\gamma-1)/\gamma+1\}]^{(\gamma+1)/(\gamma-1)}$ .

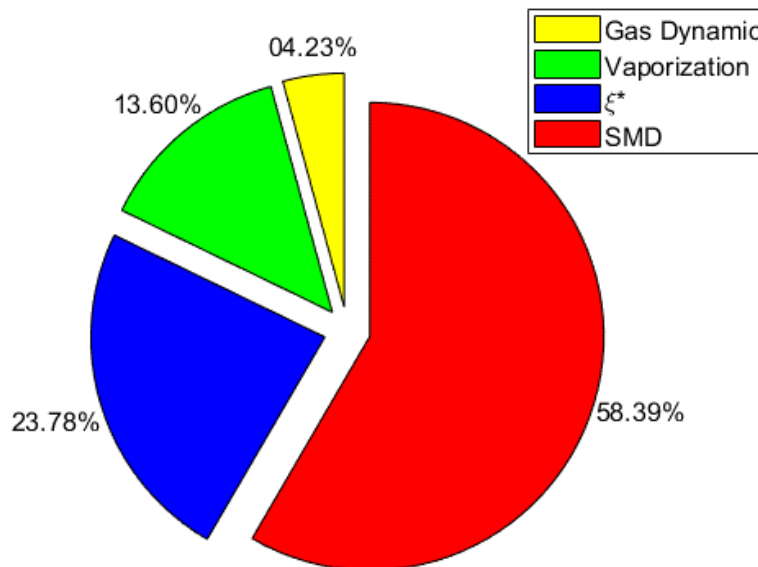


Figure 4. Comparison of the factors affecting the characteristic length

Taking in consideration the pie chart of the Fig. 4, a highly atomized propellant is the main approach for targeting a lower characteristic length. Taking this in consideration, it is clear that the design of the injector has direct impact on the  $L^*$  in 58.39 % and partial impact in the 23.78 % slice, since it directly affects the  $SMD$  and the  $\xi^*$  through the  $u_0$ . It is also possible to confirm that the chamber pressure highly impacts on the  $L^*$ , since its increase reduces the  $SMD$ , affects the  $\xi^*$  due to the impact on the injection and gas velocities, it diminishes the  $c_p$ , dropping the vaporization term, and it increases the velocity of sound  $[(\gamma RT_c)^{1/2}]$  and the gas density.

More simulations were made with the A4 varying the same parameters as the ones shown above on Figs. 1, 2, and 3. Comparing the simulations from L75 engine and the A4, it was observed that the optimum equivalence ratio, in terms of the characteristic length, is of about 0.779 for both cases, which corresponds to the L75 engine. Taking this in account, more simulations with RP-1 were made in order to investigate this result. And this phenomenon was observed as well, but for an equivalence ratio of about 1.632, which corresponds with the equivalence ratio used on previous engines such as F-1, S-4(MA-3), H-1, and RS-27 (Hugh, 1995). The equivalence ratio to reach the minimum characteristic length is

presented here as  $\Phi^*$ , named as characteristic equivalence ratio. Figure 5 presents an analysis of the characteristic equivalence ratio in terms of the chamber pressure for the two propellant mixtures studied in this work.

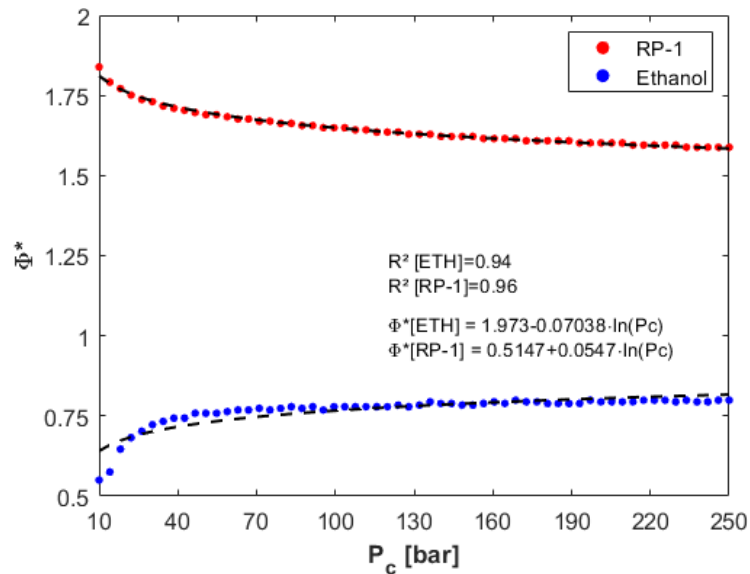


Figure 5. Characteristic equivalence ratio for Ethanol [ETH]/LOx and RP-1/LOx

As it is perceptible, the chamber pressure has low impact on the  $\Phi^*$  and logarithmic regressions were able to fit the data, facilitating a preliminary selection of  $\Phi$ .

#### 4. CONCLUSIONS

This work presented a theoretical study of the characteristic length using for Ethanol/LOx and RP-1/LOx propellant mixtures, for different chamber pressures and mixture ratios, and employing the Radcliffe and Jasuja *SMD* models for pressure swirl injectors. The results showed that the  $L^*$  decreases with the rise in chamber pressure and decrease of the propellant mass flux. With this analysis, costs, and weight savings are feasible. Additionally, performance losses are decreased. And finally, is possible to check that, in same conditions, the  $L^*$  of ethanol is higher than RP-1 combined with LOx. It was also demonstrated that an analytical approach to calculate the characteristic length is fast and low computational costly, and, consequently, minimizes the number of tests to reach the optimum experimental  $L^*$ . And this theory is important specially because tabulated data should not be used for all engines and conditions, since these data does not cover all operating conditions and losses may be too large.

The results were validated using the engines Agregat 4, F-1, and an old version of the L75, describing well the characteristic length for these engines, and presenting coherent values for the ranges tested for the actual version of the L75 engine. With these validations, it is shown that the algorithm has great accuracy with both propellant mixtures for a wide mixture ratio and chamber pressure ranges. In addition, in general, using the Radcliffe model the prediction of the  $L^*$  was more accurate than using the Jasuja model. Also, it was presented that the *SMD* has close to 58 % of impact on the  $L^*$ , representing the most important factor on determining the characteristic length in LPREs. The injector design has more than 60 % of impact, due to its importance on the *SMD* and on minimum, dimensionless, length ( $\xi^*$ ).

A promising addition to the combustion analysis of rocket and jet engines was introduced, the characteristic equivalence ratio. It is defined as the equivalence ratio required to reach the minimum characteristic length. This parameter proved that the chamber pressure itself has low impact on the  $L^*$  and it can be represented by a logarithmic equation, making it simple to select an equivalence ratio, therefore a mixture ratio, to reach the minimum characteristic length. Analyzing this parameter, it was found that the  $\Phi^*$  is of about 0.779 and 1.632 for ethanol/LOx and RP-1/LOx, respectively, that are results similar to actual engines.

#### 5. REFERENCES

- Almeida D. S., Shimote W. K., Niwa M., "Selection of Materials for Combustion Chamber of Liquid Propellant Rocket Engine", 15th Brazillian Congress of Mechanical Engineering, Águas de Lindóia, SP, 1999.
- Almeida D.S., "Projeto Motor Foguete a Propelente Líquido L75", 7º Seminário de Projetos de Pesquisa e Desenvolvimento em Veículos Espaciais e Tecnologia Associadas, 11-13, September, São José dos Campos, SP, 2013.

- Ashgriz N., "Handbook of Atomization and Sprays, Theory and Applications", Springer, 2011.
- Bayvel L., Orzechowski Z., "Liquid Atomization", Combustion: An International Series, 1 Ed., Taylor & Francis, 1993.
- Bazarov V., Vigor Y., Puri P., "Design and Dynamics of Jet and Swirl Injectors, Liquid Rocket Thrust Chambers: Aspects of Modeling, Analysis, and Design", American Institute of Aeronautics and Astronautics, 2004.
- Chickos J. S., Zhao H., "Measurement of the Vaporization Enthalpy of Complex Mixtures by Correlation-Gas Chromatography, The Vaporization Enthalpy of RP-1, JP-7, and JP-8 Rocket and Jet Fuels at T=298.15 K", Energy & Fuels, 2064-2073, 2005.
- Counsell J. F., Fenwick J., O., Lees E. B., "Thermodynamic Properties of Organic Oxygen Compounds 24. Vapour Heat Capacities and Enthalpies of Vaporization of Ethanol, 2-methylpropan-1-ol, and Pentan-1-ol", The Journal of Chemical Thermodynamics, 1970.
- Dong J. Q., Lin R. S., Yen W. H., "Heats of Vaporization and Gaseous Molar Heat Capacities of Ethanol and the Binary Mixture of Ethanol and Benzene", Canadian Journal of Chemistry, 783-790, 1988.
- Fischer G. A. A., "Injetores Centrífugos Duais e Jato-Centrífugos para Aplicação em Propulsão de Foguetes", Master's Dissertation, INPE - National Space Research Institute, 2014.
- Fischer G. A. A., Andrade J. C., Costa F. S., "Spray Cone Angles by a Pressure Swirl Injector for Atomization of Gelled Ethanol", 24th ABCM International Congress of Mechanical Engineering, December, 3-8, Curitiba, PR, Brazil, 2017.
- Fischer G. A. A., "Atomização de Géis por Injetores Centrífugos e Jato-Centrífugos para Aplicações em Propulsão de Foguetes", Doctoral Thesis, INPE - National Space Research Institute, 2019.
- Gonçalves F. A. M. M., Trindade A. R., Costa C. S. M. F., Bernardo J. C. S., Johnson I., Fonseca I. M. A., Ferreira A. G. M., "PVT, Viscosity and Surface Tension of Ethanol: New Measurements and Literature Data Evaluation", The Journal of Chemical Thermodynamics, 1039-1042, 2010.
- Haidn O. J., "Advanced Rocket Engines", In Advances on Propulsion Technology for High Speed Aircraft, 6-40, 2008.
- Hulka J., Forde J. S., Werling R. E., Anisimov V. S., Kozlov V. A., Kositsin I. P., "Modification and Verification Testing of a Russian NK-33 Rocket Engine for Reusable and Restartable Applications", American Institute of Aeronautics and Astronautics, 1998.
- Hill P., Peterson C., "Mechanics and Thermodynamics of Propulsion", Addison Wesley Longman, 2nd Ed. Sep 1, 1992.
- Hugh B. Mc., "Numerical Analysis of Existing Liquid Rocket Engines as a Design Process Starter", 31st, AIAA/ASME/SAE/ASEE Joint Propulsion Conference, July, San Diego, CA, 1995.
- Humble R. W., Henry G. N., Larson W. J., "Space Propulsion Analysis and Design", McGraw-Hill, Sep 1, 1995.
- Huzel D. K., Huang D. H., "Modern Engineering for Design of Liquid-Propellant Rocket Engines", American Institute of Aeronautics and Astronautics, 1992.
- Jasuja A. K., "Atomization of Crude and Residual Fuel Oils", ASME J. Eng. Power, Vol 101, No.2, pp. 250-258, 1979.
- Kang Z., Wang Z., Li Q., Cheng P., "Review on Pressure Swirl Injector in Liquid Rocket Engine", Acta Astronautica, 145, 174-198, 2018.
- Kessaev J. V., "Theory and Calculation of Liquid-Propellant Engines", Moscow Aviation Institute, Feb-Apr, 1997.
- Khavkin Y. I., "Theory and Practice of Swirl Atomizers", CRC Press, 1 Ed., 2003.
- Lefebvre A. H., McDonell V. G., "Atomization and Sprays", Taylor & Francis Group, LLC, 2017.

- Magee J. W., Bruno T. J., Friend D. G., Huber M. L., Laesecke A., Lemmon E. W., McLinden M. O., Perkins R. A., Baranski J., Widgren J. A., "Thermophysical Properties, Measurements and Models for Rocket Propellant RP-1: Phase I", National Institute of Standards and Technology, NISTIR 6646, 2007.
- McBride B. J., Gordon S., "Computer Program for Calculating and Fitting Thermodynamic Functions", NASA Reference Publication 1271, 1992.
- McBride B. J., Gordon S., "Computer Program for Calculation of Complex Chemical Equilibrium Compositions and Applications", NASA Reference Publication 1311, Part I: Analysis, 1994.
- McBride B. J., Gordon S., "Computer Program for Calculation of Complex Chemical Equilibrium Compositions and Applications", NASA Reference Publication 1311, Part II: Users Manual and Program Description, 1996.
- Mota F. A. S., Hinckel J. N., Rocco E. M., Schlingloff H., "Modeling and Analysis of a LOX/Ethanol Liquid Rocket Engine", Journal of Aerospace Technology Management, V. 10, 2018.
- Pfuetzenreuter L., Burkhardt H., Lippert C., Wagner B., Almeida D. S., Pagliuco C. M. M., Nascimento L. B., Souza B. R. D., Zink E. Araujo T. B., Alting J., Preuss A., Langel G., "L75 LOx Ethanol Engine: Current Status of Thrust Chamber and Turbopump Cooperative Development", 53rd, AIAA/SAE/ASEE Joint Propulsion Conference, July, Atlanta, Ga, 2017.
- Radcliffe A., "Fuel Injection", High Speed Aerodynamics and Jet Propulsion, Vol XI, sect. D, Princeton, 1960.
- Rizk N. K., Lefebvre A. H., "Internal Flow Characteristics of Simplex Swirl Atomizers", Journal of Propulsion and Power, Vol. 1, No. 3, May-June, 1985.
- Saeedipour M., Schneiderbauer S., Pirker S., Bozorgi S., A Numerical and Experimental Study of Flow Behaviour in High Pressure Die Casting, Magnesium Technology, 185-190, 2014.
- Salvador C. A. V., Costa, F. S., "Vaporization Lengths of Hydrazine Fuels Burning with NTO", Journal of Propulsion and Power, Vol. 22, No. 6, 2006.
- Salvador C. A. V., "Modelo Matemático de Câmaras de Combustão Bipropelentes", Masters Dissertation, INPE - National Space Research Institute, 2004.
- Schmidt P., Walzel P., "Zerstäuben von Flüssigkeiten", Physik in Unserer Zeit, 113-120, 1984.
- Spalding D. B., "The Combustion of Liquid Fuels", Symposium (International) on Combustion, 1953.
- Spalding D. B., "Combustion in Liquid-Fuel Rocket Motors", Imperial College of Science and Technology, London, 1958.
- Spalding D. B., "A One-Dimensional Theory of Liquid-Fuel Rocket Combustion", Ministry of Supply Aeronautical Research Council, Imperial College of Science and Technology, London, 1959.
- Spalding D. B., "Combustion and Mass Transfer: A Textbook with Multiple-Choice Exercises for Engineering Students", Pergamon Press, 1979.
- Sutton G. P., Biblarz O., "Rocket Propulsion Elements", John Wiley & Sons, 2010.
- Torres M. F. C., Almeida D. S., Krishna Y. S. R., Silva L. A., Shimote W. K., "Propulsão Líquida no IAE: Visão das Atividades e Perspectivas Futuras", Journal of Aerospace Technology and Management, V. 1, n. 1, Jan, 2009.
- Vijay G. A., Moorthi N. S. V., Manivannan A., "Internal and External Flow Characteristics of Swirl Atomizers: A Review", Atomization and Sprays, 153-188, 2015.
- Wang Z. G., "Internal Combustion Processes of Liquid Rocket Engines: Modeling and Numerical Simulations", National Defense Industry Press, Wiley, 2016.

## 6. RESPONSIBILITY NOTICE

The authors are the only responsible for the printed material included in this paper.